An Experimental Analysis of High-Speed-Distance Protection

Cezary Dzienis
E D EA D
Siemens AG
Berlin, Germany
cezary.dzienis@siemens.com

Matthias Kereit
E D EA D
Siemens AG
Berlin, Germany
matthias.kereit@siemens.com

Jörg Blumschein
E D EA D
Siemens AG
Berlin, Germany
joerg.blumschein@siemens.com

Michael Claus
E D EA PRO
Siemens AG
Nürnberg, Germany
michael.claus@siemens.com

Abstract—**In this paper the High-Speed-Distance Protection algorithm will be discussed. The principle of this novel function is based on the so called dynamic delta-quantities resulting from splitting the electrical circuit after a short circuit event by means of the superposition technique. Due to fact that the estimation of the fault localization takes place in a time domain, the algorithm presents a good alternative to the conventional distance protection, where response speed of the relay plays an important role (high voltage network). The test results of the High-Speed-Distance will be discussed and application areas of this function presented.**

Keywords: Protection System, High-Speed-Distance, Loop Selector, Directional Element, Distance Element, Testing the Distance Protection

I. INTRODUCTION

The electrical short circuit is one of the most dangerous phenomena in power systems. It results in system instability and, in the worst case, outage. Therefore, it is imperative that short circuits be selectively eliminated from the system operation. This task is taken over by the protection devices [1]-[2]. Especially in high voltage networks, stability must be ensured by fast protection systems, which allow for detection and clearance of the faults in as short a time as possible. Since the high voltage networks often distribute energy over hundreds of kilometers, the most popular fault detection instrument for this voltage level is the so called distance protection. Amongst others, its significant advantage is that it can be installed at any network node and can work autonomously to protect or be responsible for a specific network line. The communication with other devices is not necessary here. The principle of the common distance protection is to measure short circuit impedance in the electrical loop containing the fault and, based on this information, the protection device should decide if the short circuit is localized in so called protected zones applied with the settings [1]-[3]. The impedance measurement process has a negative influence on the tripping time and thereby on the system operation [4]. In this article a further method for the short circuit distance estimation will be presented. The estimation of the fault location takes place by analyzing the samples. As a result of the estimative nature with regard to the fault location contained in the described method, it can attain significantly faster operation compared with conventional distance protection. Therefore, this computation technique is called High-Speed-Distance (HSD). The procedure is based on delta-quantities which reflect the electrical state change in the network due to the short circuit event [5]. The paper will discuss the theoretical background of the method. Detailed discussion of the sensitivity of the function will be carried out as well. The method was successfully implemented in a prototype device, and the response of the algorithm to different fault types will be presented. The test version of the algorithm was successfully tested on a complex hardware network model. Thus, the acquired results of the algorithm responses are representative and comparable with a practical application.

II. BACKGROUND OF THE METHOD

A. Theoretical Consideration

As already mentioned, the electrical fault at the line is a dangerous event that results from rapid, undesirable change in the physical network structure with a significant impact on the energy transmission in entire system. Because of that, such phenomenon should be recognized as quickly as possible and then the faulty network area eliminated from system operation. To do so the conventional distance protection has been designed, the task of which is to measure the impedance of the fault contained in the electrical loop and to compare it with the impedance settings that define the operation range of the protection. In order to calculate impedance the following simplified expression, based on Figure 1, can be applied:

$$a\underline{Z}_L = \frac{f_{\cos}[u_A] + j \cdot f_{\sin}[u_A]}{f_{\cos}[i_A] + j \cdot f_{\sin}[i_A]}, \qquad (1)$$

where a$\underline{Z}$L is the fault impedance f_{cos}, and f_{sin} are the cos and sin filters respectively. The response time of the (1) depends on the filter length. Therefore, time performance of this method is limited mostly by the applied filter length. Normally the calculation technique to determine the short circuit impedance can require more samples than those contained in the half cycle interval of the fundamental period of the system. Depending on the short circuit location and conditions before short circuit occurred, the number of samples required is sometimes more than those in one or two fundamental cycles [4]. Therefore, another method with better performance can be applied. Namely, by analyzing the situation before and after the fault event, the exact fault localization can be carried out without needing to determine the short circuit impedance. This method is based on so called delta-quantities. The principle of the

method can be considered based on the simplified single phase system given in Figure 1. In this case the fault is represented as the closing of the switch K. The protected line exists between points A and B with line impedance of $\underline{Z}_L$. The system is supplied by two sources $\underline{E}_{S,A}$ and $\underline{E}_{S,B}$ with certain short circuit power characterized by the source impedances $\underline{Z}_{S,A}$ and $\underline{Z}_{S,B}$. The fault is placed in such a way that the calculated impedance from measurement point A equals $a\underline{Z}_L$ and from point B equals $(1-a)\underline{Z}_L$. Since the distance protection is an autonomous device that does not need communication with another end, the consideration can be performed from just one point, e.g. A only. From the superposition principle applied to linear networks, the electrical system from Figure 1 after closing switch K, can be split into two networks as given in Figure 2 and Figure 3. This is possible if the closing of switch K is modeled as a series connection of two equivalent voltage sources u_K with opposite sign and if the magnitude equals the voltage at the location of the short circuit before the short circuit occurred [5]-[6].

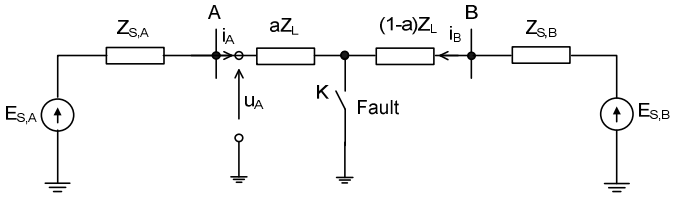

Figure 1. Schematical representation of electrical circuit structure change after fault on the line

The network in Figure 2 reflects system operation as if short circuit didn't happen. It defines the so called pre-fault conditions. The equivalent voltage u_K doesn't influence the voltages and currents in this network because this equivalent voltage equals the potential at the location of the short circuit. Figure 3 represents the system operation accompanying the short circuit event. In this case the equivalent voltage source u_K has significant influence on the voltages and currents in the considered system (fault condition). Since other active elements are short circuited and applied in the previous network system (Figure 2) only this source produces the currents and voltages. Appling the superposition method to these two circuits the following equation can be arranged [7]:

$$\begin{aligned} u_A(t) &= u_{p,A}(t) + \Delta u_{f,A}(t) \\ i_A(t) &= i_{p,A}(t) + \Delta i_{f,A}(t) \end{aligned}, \qquad (2)$$

where $u_A(t)$, $i_A(t)$ are measured voltage and current at point A. The $u_{p,A}(t)$ and $i_{p,A}(t)$ are quantities which reflect pre-fault conditions. The $\Delta u_{f,A}(t)$, $\Delta i_{f,A}(t)$ delta-quantities represent fault conditions with decoupling of the load flow.

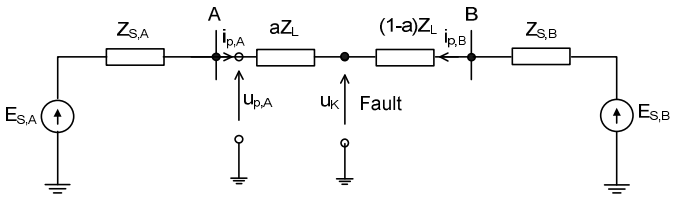

Figure 2. Schematical representation of an electrical circuit in the form of the pre-fault quantities

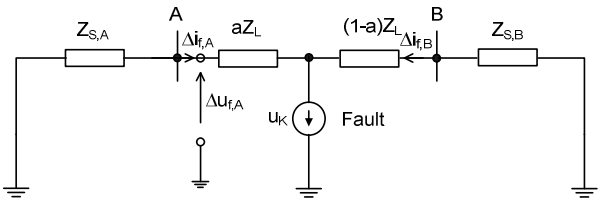

Figure 3. Schematical representation of the electrical circuit in the form of the delta-quantities

The curves of the calculated currents and voltages for given circuits are presented in Figure 4. The pre-fault quantities $u_{p,A}(t)$, $i_{p,A}(t)$ are still constant in reference to magnitude and phase. However delta-quantities reflect the voltage and current changes in comparison to the previous network state. Therefore strong changes can be observed. Additionally, an angle of about 90° (short circuit impedance angle) between these quantities appears. This is due to the fact that the short circuit loop has a strong inductive component. As can be seen from the equivalent circuit in Figure 2, the localization of the fault can not be carried out. The gathered quantities from this circuit do not generate a new contribution to the network operation. They still carry information according to the load conditions. On the other hand, the delta-quantities resulting from the equivalent circuit in Figure 3 deliver completely new information resulting from the short circuit impact. They can be used for detection of the fault position in the network [6]-[7].

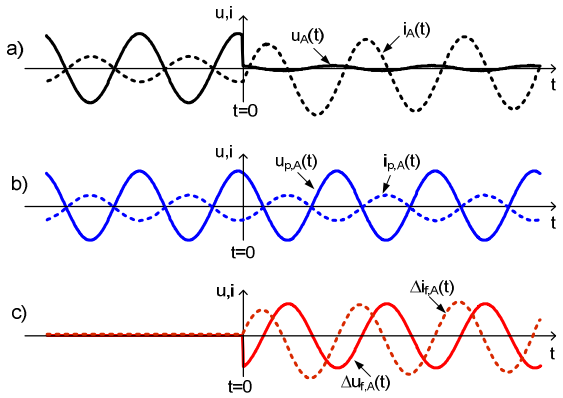

Figure 4. Electrical quantites during fault event: a) voltage and current before and after short circuit; b) voltage and current without short circuit; c) delta-voltage and delta-current.

The calculation of the pre-fault currents $i_{p,A}(t)$, pre-fault voltages $u_{p,A}(t)$, delta-voltages $\Delta u_{f,A}(t)$ and delta-currents $\Delta i_{f,A}(t)$ can be carried out if the network structure and its parameters are known. In a normal case, only the measured values after and before short circuit are available. Therefore the relevant delta-quantities can be approximated based on fault and pre-fault values of $i_A(t)$ and $u_A(t)$ as expressed in (3):

$$\begin{aligned} \Delta u_{f,A}(t) &\approx u_A(t) - u_A(t-T) \\ \Delta i_{f,A}(t) &\approx i_A(t) - i_A(t-T) \end{aligned}, \qquad (3)$$

where T is the fundamental period. The $u_A(t\text{-}T)$ and $i_A(t\text{-}T)$ are close to pre-fault quantities $u_{p,A}(t)$ and $i_{p,A}(t)$. It is assumed here that behavior of the network, before short circuit happened, is

not disturbed. Otherwise this approximation is afflicted with relatively significant errors. To avoid the error for frequency deviation a more complicated approximation technique for creating delta-quantities must be realized.

B. High-Speed-Distance Function

Three particular modules create the High-Speed-Distance protection function. These are: loop selector, directional element and distance element. In addition, the other functions must be implemented that have the task to stabilize the function due to disturbances or diverse non-conformed network states. The cases where the stabilization rules are needed and also justified will be presented in section III.

Based on the delta-quantities the faulty loop can be selected. Particularly, such selection takes place by analyzing the delta-currents and delta-voltages. Investigations of the delta-phase-to-phase quantities for both current and voltage are very useful for this task as well. For example, based on the delta-phase-to-phase currents it can be very easily differentiated between single and multiple pole faults, and the phases in which the fault occurred can be detected. The following statement results from such consideration: for a single-phase fault the delta-current for healthy phases is close to zero; if the double phase fault appears then the delta-phase-to-phase current in unhealthy phases is much larger than other phase-to-phase delta-currents; in case of the three phase fault all phase-to-phase delta currents are equal to each other. Since the loop selector must decide in a short time which loop is defective, the confirmation of the faulty loop must be carried out. This can be realized by means of the delta-voltages, graphically shown in Figure 5.

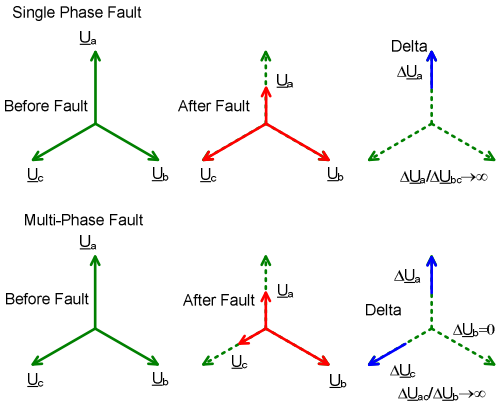

Figure 5. Loop selection based on the delta-voltage

For example, if a single pole fault appears the voltage breaks down in the defective phase and the ratio between the delta-voltage in the defective phase to the delta-phase-to-phase voltage in the healthy phases is high. In the case of a recognized two-pole short circuit the ratio between the unhealthy phase-to-phase and the non-defective phase is investigated. If this ratio is high the phase-to-phase loop is confirmed. For three-phase faults the ratios between phase-to-phase voltages are equal to each other. Such a two step loop selector creates a very robust element. Analyzing delta-quantities, it can be concluded that the calculated impedance according to (1) allows for detection of the direction of the fault:

$$\Delta\underline{Z} = \frac{f_{\cos}\left[\Delta u_{A,f}\right] + j \cdot f_{\sin}\left[\Delta u_{A,f}\right]}{f_{\cos}\left[\Delta i_{A,f}\right] + j \cdot f_{\sin}\left[\Delta i_{A,f}\right]}, \tag{4}$$

where $\Delta\underline{Z}$ is the impedance acquired from delta-quantities. $\Delta\underline{Z}$ equals to $-\underline{Z}_{S,A}$ (negative impedance) if the fault is in a forward direction or $\underline{Z}_{S,B}+\underline{Z}_L$ (positive impedance) if the fault is localized in a reverse direction. Since the calculation of the impedance $\Delta\underline{Z}$ doesn't bring any advantages in comparison to the method of the conventional distance protection (the response speed depends still on the filter length), only impedance sign must be predicted. The prediction is based on the assumption of the so called replica impedance $\underline{Z}_R$ [8]-[9] that should be close to the back source impedance $\underline{Z}_{S,A}$. Equation (5) shows the acquiring process of the delta-voltages in a schematic way:

$$\begin{aligned} \Delta u_f &= \Delta u_{f,A} \\ \Delta u_R &= \underline{Z}_R \circ \Delta i_{f,A} \end{aligned}, \tag{5}$$

where $\underline{Z}_R$ is assumed replica impedance. A denotes the measurement point in the system (station A). The expression is valid for single phase representation of the system given in Figure 1. The calculation should take place in the time domain in which the $\underline{Z}_R$ is replaced by the differential operator in form of $(L_R d/dt + R_R)$. The acquired quantities create the trajectories, which for forward fault are placed in quadrants II and IV of the Δu_R, Δu_f plane. Also, the trajectory circulates in a positive clockwise direction. For reverse fault, the trajectory is localized in quadrants I and III. It rotates in a negative clockwise direction. The usage of the replica impedance $\underline{Z}_R$ allows for transformation of the delta-current Δi_f in such way that occurred trajectories from both delta-voltages Δu_R, Δu_f are very well defined. If only delta-voltage Δu_f with delta-current Δi_f are taken into consideration, the computed trajectory is placed in all quadrants and the fault direction can be detected based on recognizing the rotation sense and position trajectory in the initial condition (fault begin). Since the fault quantities include the distortion or, e.g., DC components this is definitely not a secure instrument [7].

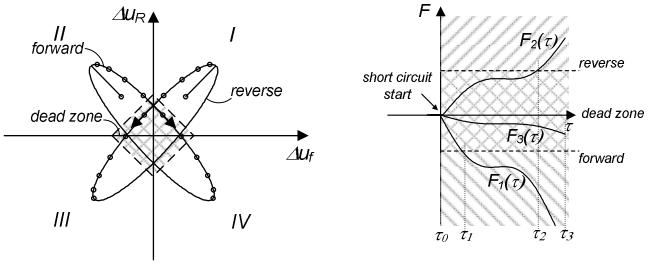

Figure 6. Trajectories and curves of the directional element based on delta-quanities

The possible trajectories for these two fault directions are presented in Figure 6. Generally they have approximately an elliptical shape that results from differences between assumed replica impedance $\underline{Z}_R$ and real appeared impedance calculated in the form of delta-impedance $\Delta\underline{Z}$. If the angle of the assumed replica impedance $\angle\underline{Z}_R$ is close to the angle of delta impedance $\angle\Delta\underline{Z}$ the ellipse form aspires to be a straight line. If additional magnitudes of both impedances are the same, a straight line

with the slope of 45° appears. Since in the range of small delta-quantities, high uncertainty appears, (e.g. mostly measurement error) the so called dead-zone must be introduced. It contributes certain limitation to the method that can be annulled if the delta-voltages are simply filtered by an integral function in the following way [8]-[10]:

$$F(\tau) = \int_0^{\tau} \Delta u_f(t) \cdot \Delta u_R(t) dt \,. \tag{6}$$

If the function F(τ) is negative (for $\tau=\tau_1$) then forward fault will be concluded. For the reverse fault a positive integral function F(τ) (for $\tau=\tau_2$) should appear. The uncertainty of the method is then reflected by the non directional area as presented in Figure 6. Depending on the availability of the fault quantities after short circuit, the given threshold for reverse or forward fault recognition can vary. The replica impedance $\underline{Z}_R$ is the main factor that has impact on the sensitivity of this direction estimation method. Thereby two components play central role: there is magnitude and angle of the replica impedance $\underline{Z}_R$. The magnitude can contribute so called under-function only, e.g. if the chosen magnitude for replica impedance is too low. However, significant deviation of the angle from the real delta-impedance $\Delta\underline{Z}$ can introduce over-function. The influence is presented in Figure 7 and Figure 8.

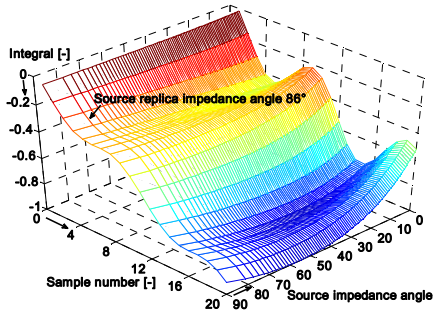

Figure 7. Sensitivity of the direction method for a different replica impedance angle

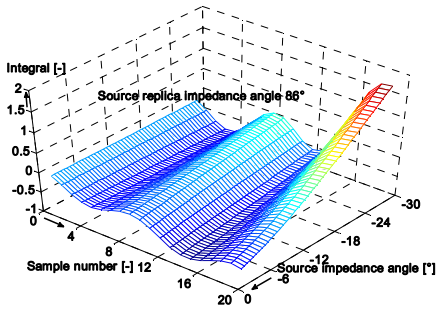

Figure 8. Sensitivity of the direction method for a different replica impedance angle

It was assumed here that the replica impedance $\underline{Z}_R$ has a constant angle of 86°. Also, the forward fault was simulated in a network with a different angle of reverse source impedance. The angle of this impedance varied between 90° (inductive) and -30° (capacitive). It can be noted that even if angle deviation is big, the integral curve has correct tendency. Only the oscillated form can be observed. If the source impedance is capacitive then the curve develops in the defective opposite direction. This results from the fact that, the assumed model for delta-voltage calculation is not matched with the physical condition in the network. Since the source impedance is inductive and the line impedance, also by series compensated line, is inductive as well, the direction calculation can be interpreted as a stable method. In the normal case (three phase system) delta-voltages are calculated for the defective phase/phases. As a result, a directional element is activated for the faulty loop only. The six loops are not calculated in parallel. Which loop is activated, depends on the signal from the loop selector, shortly described above. For the phase-to-phase defective loops the delta-voltages u_f and u_R are created from phase-to-phase voltages and currents respectively. For the phase-earth loops, the delta-voltages u_f and u_R are built from phase-to-earth voltages and phase currents respectively. Since the loop in the phase-earth mesh is inductive, the earth current with appropriate influence of the replica zero-sequence impedance $\Delta\underline{Z}_0$ is not taken into account because it insignificantly influences the directional element algorithm (see general consideration in Figure 7 and Figure 8). Besides this replica zero-sequence impedance $\Delta\underline{Z}_0$ is unknown and similar to the common line replica impedance $\underline{Z}_R$ must be assumed. It can be an additional error source. The mutual coupling also has low influence on the directional element, because during this effect the loop character is still inductive and consideration from Figure 7 and 8 can be applied.

The calculation of the fault localization is based on the comparable analysis of the equivalent voltage u_K at the location of the short circuit. Since this location is unknown, the reference voltage u_{ref} must be calculated. This voltage results from the theoretical voltage at the end of the protected zone as if the fault would appear exactly at end of the protected zone. Hereby, the protected zone is characterized by high-speed-distance impedance (HSD) $\underline{Z}_{HSD}$, particularly lower then the line impedance $\underline{Z}_L$. Applying Kirchhoff's laws for equivalent circuit resulting from the superposition principle (Figure 2), the reference voltage u_{ref} can be expressed as follows (7):

$$u_{ref} = u_{p,A} - \underline{Z}_{HSD} \circ i_{p,A}\,, \tag{7}$$

where $\underline{Z}_{HSD}$ is the differential operator in form of ($L_{HSD}d/dt + R_{HSD}$). Usage of this differential operator allows for calculation of the reference voltage u_{ref} in the time domain. The index A denotes the measurement point in the network (in this case the station A). It must be noted here that all computations must be preformed in the time domain. In the normal case, formula 7 must be fitted into an appropriate defective electrical loop that is annunciated by the phase selector. Hereby the differences in equation between single-pole short circuit to earth and multiple pole phase faults appear. Expression 7 presents the simplification that is valid for the single-phase system if, additionally, the earth line impedance is equal to zero. For double-phase and three-phase faults the phase-to-phase loop is selected and calculation takes place on phase-to-phase quantities for voltage and current respectively. When the phase-earth loop is selected, the appropriate phase-to-earth voltage with suitable phase current and earth current is involved in the calculations. In such case the expressions from 7 and 8 must be completed with the zero-sequence

compensation factor that reflects non-homogeneity between phase and earth impedances. Since the selector chooses one loop only, only one loop is calculated by the distance element. The equivalent voltage at the end of the high-speed-distance zone can be also calculated from delta-quantities (see section II) like (8):

$$u_{HSD} = -\Delta u_{f,A} + \underline{Z}_{HSD} \circ \Delta i_{f,A} \,. \tag{8}$$

In order to detect where the fault is localized, comparison between these two voltages, u_{ref} and u_{HSD}, must be carried out. Thereby, the following conclusions can be made:

- if $u_{HSD} > u_{ref}$ then the equivalent source u_K must be situated in the zone $\underline{Z}_{HSD}$, (internal fault)
- if $u_{HSD} < u_{ref}$ then the equivalent source u_K must be situated outside zone $\underline{Z}_{HSD}$ (external, forward or reverse fault)
- if $u_{HSD} = u_{ref}$ then the equivalent source u_K is situated exactly at the zone $\underline{Z}_{HSD}$ (fault at zone limit)

In order to achieve good stability of the distance element with good time performance the calculation of the voltages u_{HSD} and u_{ref} is realized by means to of the average rectified values. These values are obtained in the moved constant window with the length of the half of fundamental period. Since the building of the average rectified value for the voltage u_{kHSD} is not always possible, the missing samples of the voltage u_{kHSD} are replaced by samples of the u_{ref}. This happens only for the short time after fault. Additionally, the dynamic pick-up characteristic for distance element is applied, that introduces stabilization in case of disturbances which can be amplified by the derivation element in expression 7 and 8.

The sensitivity investigation of the distance prediction method based on delta-quantities can be performed using the complex static values. At first the situation of the fault in forward direction will be considered. From a measurement point of view the complex equivalent voltage source can be computed as given in (9). For this task the equivalent circuit from Figure 3 should be applied:

$$\begin{aligned} \underline{U}_K &= -\Delta\underline{U}_{f,A} + \Delta\underline{I}_{f,A} \cdot \underline{Z}_f = \Delta\underline{I}_{f,A} \cdot (\underline{Z}_{S,A} + \underline{Z}_f) \\ \underline{U}_{HSD} &= -\Delta\underline{U}_{f,A} + \Delta\underline{I}_{f,A} \cdot \underline{Z}_{HSD} = \Delta\underline{I}_{f,A} \cdot (\underline{Z}_{S,A} + \underline{Z}_{HSD}) \end{aligned}, \tag{9}$$

where $\underline{Z}_f$ is the short circuit impedance. Since this short circuit impedance is unknown, the theoretical equivalent voltage $\underline{U}_{HSD}$ can be computed like in (8), but on complex values. As can be easy noted, if the fault impedance is lower then HSD impedance (fault in the zone), the voltage $\underline{U}_{HSD}$ is higher than voltage $\underline{U}_K$. On the other hand, voltage $\underline{U}_K$ is approximately equal to the $\underline{U}_{ref}$ computed from the equivalent circuit in Figure 2. Additionally, usage of voltages $\underline{U}_K$ and $\underline{U}_{HSD}$ allows for computation of the HSD-characteristic (10):

$$\begin{aligned} &\left|\underline{U}_{ref}\right| \approx \left|\underline{U}_K\right| \le \left|\underline{U}_{HSD}\right| \\ &(R_{S,A} + R_f)^2 + (X_{S,A} + X_f)^2 \le \left|(\underline{Z}_{S,A} + \underline{Z}_{HSD})\right|^2 \end{aligned}, \tag{10}$$

where $R_{S,A}$ and $X_{S,A}$ are parameters of the source impedance. R_f and X_f are resistance and reactance measured at the short circuit location. A circle results from this equation, see Figure 9 for which the following interpretation can be applied: the HSD-pick up characteristic is a circle with the center created by the source impedance in reverse direction $\underline{Z}_{S,A}$ and radius as the sum of the source impedance $\underline{Z}_{S,A}$ and HSD-impedance $\underline{Z}_{HSD}$. Since the fault impedance $\underline{Z}_f$ is placed in quadrant I of the complex plane, only the characteristic in quadrant I is applicable. Depending on the source impedance $\underline{Z}_{S,A}$, the distance characteristic can vary in R direction (real axis). The reach in direction of the line impedance $\underline{Z}_L$ is always constant. Therefore, the best performance of the HSD-algorithm is obtained if a metal short circuit without transition resistance appears.

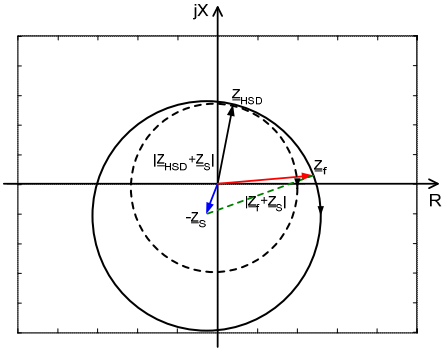

Figure 9. Distance characteristic for the forward fault (HSD-method)

Similar considerations can be carried out for the reverse faults. The mathematical equation for description of the voltage in form of $\underline{U}_K$ and $\underline{U}_{HSD}$ quantities is given in (11):

$$\begin{aligned} \underline{U}_K &= -\Delta\underline{U}_{f,A} - \Delta\underline{I}_{f,A} \cdot \underline{Z}_f \\ &= -\Delta\underline{I}_{f,A} \cdot (\underline{Z}_f + \underline{Z}_L + \underline{Z}_{S,B}) \\ \underline{U}_{HSD} &= -\Delta\underline{U}_{f,A} + \Delta\underline{I}_{f,A} \cdot \underline{Z}_{HSD} \\ &= \Delta\underline{I}_{f,A} \cdot (\underline{Z}_L + \underline{Z}_{S,B} - \underline{Z}_{HSD}) \end{aligned} \tag{11}$$

If we compare the magnitudes of both voltages $\underline{U}_K$ and $\underline{U}_{HSD}$ with each other and assume that the line impedance $\underline{Z}_L$ is approximately equal to HSD-impedance $\underline{Z}_{HSD}$ the following expression is can be written:

$$\begin{aligned} &\left|\underline{U}_{ref}\right| \approx \left|\underline{U}_K\right| \ge \left|\underline{U}_{HSD}\right| \\ &(R_{S,B} + R_L + R_f)^2 + (X_{S,B} + X_L + X_f)^2 \ge \left|\underline{Z}_{S,B}\right|^2 \end{aligned}. \tag{12}$$

Also in this case the circle characteristic is obtained. The radius of the circle equals the magnitude of the source impedance $\underline{Z}_{S,B}$ and the circle is shifted as a sum of the line and source impedance. From this characteristic it can be observed that the fault impedance $\underline{Z}_f$ cannot reach the inside of the circle (fault in HSD zone), so that no over-function for reverse fault should appear. It can be expected that that HSD algorithm behaves very stable for these fault types. The next conclusion is that the distance element includes the properties of the directional element. As a result of that the more stable directionality of the HSD-function is guaranteed. Since the HSD protection method is based on the time domain calculation, its distance estimation algorithm can exhibit some uncertainties in reference to the static characteristics from Figure 9 and Figure 10. It can especially occur, if the comparison is carried out with a low number of samples. The potential problems are discussed in next section.

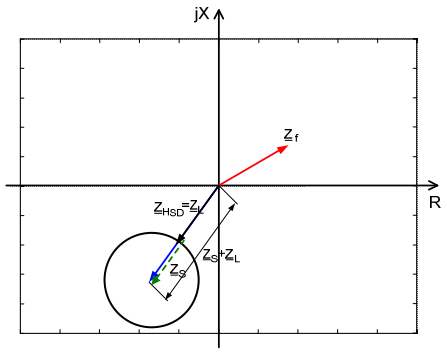

Figure 10. Distance characteristic for the reverse fault (HSD-method)

III. TEST SYSTEM AND TEST RESULTS

According to the considerations from section II, for the loop selector, directional element, distance element and other supported methods, the discrete simulation models in Matlab/Simulink were developed. Based on simulation results acquired from the real time hardware model, the expanded models were appropriately optimized so that the desired balance between performance and stability of the entire HSD-function was achieved. These models were implemented into a digital protection device and suitably fitted at its structure. The function was tested according to its behavior for different network states (mostly faults) and according to its integration level in a digital device. The test results are described in this section. The model on which the tests were performed is a scaled physical network of 500kV high voltage system. Scaling of the parameters took place with the commonly used secondary values. The advantage of such a scaled network against the RTDS network model, is that many of the different electro-magnetic effects can be included. In order to guarantee the real time simulation for the big network structure, an RTDS system uses strongly simplified models. Thereby some possible interesting phenomena (mostly with non-linear background) for protection tests can not be taken into account.

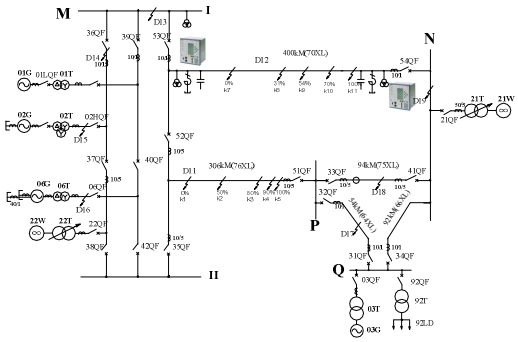

Figure 11. Test system for protection systems

Tested devices were placed at the line D12, and the following tests were performed:

- performance test
- over-function test
- evolving faults test
- power swing test
- special practice relevant tests

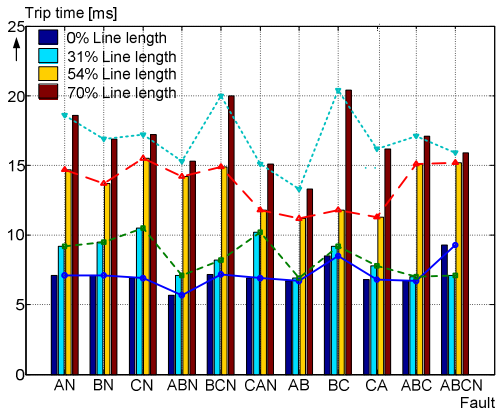

Figure 12. Results of performance test

In Figure 12 the trip times of the HSD-algorithm, for different fault types and fault localizations on the line, were presented. It can be observed that the tripping times, measured with an electronic device relay, are between 5ms and 20ms. These tripping times reflects the real response time of the algorithm with measurement uncertainty of about 1ms. For the initiated faults under 30% of the line length, the HSD-algorithm needs significantly lower than half of the fundamental period to trip. The faults from 50% up to 100% of the line length can be tripped also in fast time, namely under single fundamental period. Deviation of the tripping times for the same fault types results particularly from the fault initiation angle. The best performance of the algorithm can be achieved if this angle equals the line angle. Besides if disturbances appear, the tripping time is much higher. Analyzing the tripping times it can be noted that the HSD-function offers definitely better performance according to tripping time than a conventional distance element based on impedance calculation. Hereby it must be said that HSD is designed to trip clear interpretable faults on the line. Therefore, this function should operate in cooperation with conventional distance elements that allow for tripping of the faults with high complexity. The usage of the HSD-function can be definitely confirmed if it responds only when forward fault appears on the protected line. Therefore the algorithm was tested according to potential over-functions. Hereby, the following faults outside the protected zone were initiated on the model: reverse faults, faults on the limit of the HSD zone, faults on a parallel line, faults during week in-feed, external faults during frequency deviations as well as external faults with significant disturbance content. In order to show the intensity of the tests according to the over-function two cases were graphically presented. In Figure 13 the forward fault outside the zone with significant disturbance content was plotted. For the fast distance function (HSD) based on time domain calculation, the appeared disturbances during short circuit event can be especially dangerous, because the signal processing is limited to a very short pre-processing filter, mostly anti-aliasing filter only. Since for the distance estimation procedure a derivative operator is applied, the disturbances can be amplified and therefore an overreach of the distance function can appear. This eventually effect can be recognized in Figure 13. The voltage curve u_{HSD} acquired from delta-quantities exhibits strong deviation from the fundamental component of 50Hz sinus wave. For some samples this curve

exceeds the reference voltage u_{ref}. Hereby it can be suggested that the fault is inside the HSD-zone and a defective trip can happen. Based on this example it can be concluded that prevention of the overreach effect during the disturbances is a big challenge for the HSD-function.

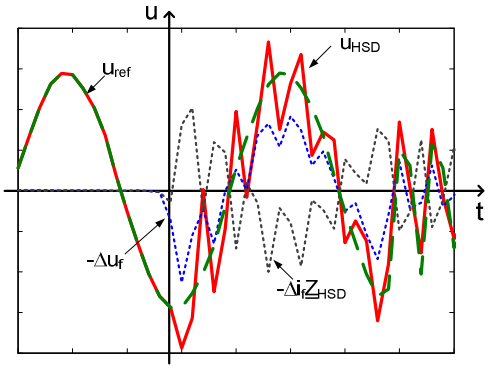

Figure 13. External Fault at >100% line length with significant disturbances content

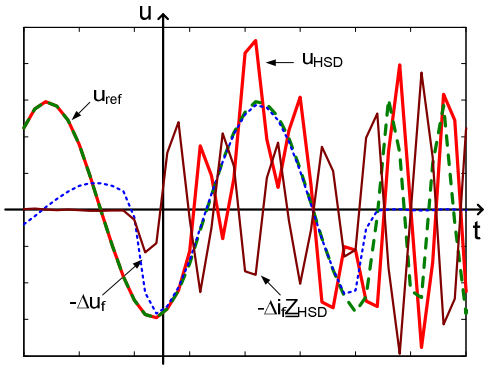

Figure 14. Reverse fault with significant disurbance content

In Figure 14 disturbance problems for the reverse fault are shown. This is a more complex situation than the overreach effect in the case of the forward fault. Because of significant disturbances defective direction of the short circuit can be detected. Since for reverse fault close to the measurement point the voltage breaks completely down (significant delta voltage quantities) and additionally the short circuit current is strongly disturbed, the directionality of the distance element can not be guaranteed any more. Then the mis-operation of the HSD-function can happen. Such potential effect of the disturbances impact is presented in Figure 14. The reference voltage u_{ref} is exceeded repeatedly by the voltage u_{HSD}. In order to stabilize the response of the algorithm in case of the disturbances, a special method was developed that detects the distortions in a short time and either blocks the HSD-function completely or introduces an appropriate stabilization threshold. This depends on the force of the disturbances. The method is based on the investigation of the function monotony in an available calculation window. The disturbance detection method combined with the main HSD function creates a very stable high speed distance protection. Therefore, usage of the HSD is also confirmed in a network with significant disturbance content. Since in the high voltage networks, so called evolving faults can happen, the HSD-function was programmed in such way that its operation during these fault types is possible as well. The performance of the method according to the tripping time is also very good. This is shown in Figure 15. The transferring of the reverse to forward fault was simulated. In most cases the tripping time took place in less than half of the fundamental period. The only time the HSD-algorithm didn't trip after 20ms was for the evolving fault BCN. This is due to the occurred condition according to the earth current. Moreover, the other fault transferring possibilities were tested like: internal to internal and internal to external fault with different delay times. The HSD-function operates very stable and no over-function is detected.

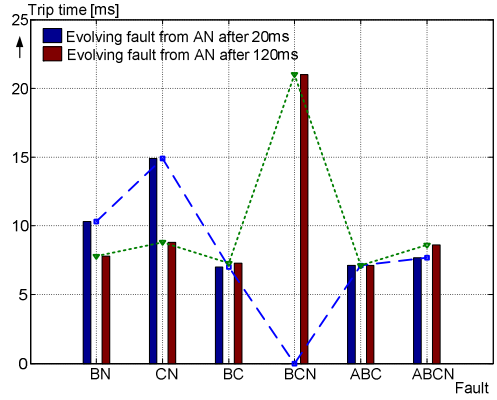

Figure 15. Results of the evolving fault tests

The interesting case of the fault transferring from external to internal during the same phase is presented in Figure 16. At first the reverse fault was initiated and after 20ms the forward fault was started. After reverse fault, the directional element recognized reverse fault and the distance element was not activated. Nevertheless the distance element exhibits also correct directionality. The u_{HSD} curve is lower than reference voltage u_{ref}. After forward fault with a delay of 20ms the voltage curve u_{HSD} exceeds the reference voltage u_{ref} and a single pole trip happens. From this consideration it can be concluded that the HSD-function can be used for clearance of evolving faults as well. Excellent performance according to the tripping time and stability of the HSD-function enlarges its application area to these fault types. This is very important because generally the tripping time of the conventional distance protection is a little bit higher for the evolving faults than for the simple faults. The power swing phenomenon is relative frequently occurring state in the power system. Detailed tests were performed for this phenomenon as well. Three important reactions must be expected from HSD to make it applicable as distance protection: no over-function during a pure power swing, no over-function during an external fault that is combined with a power swing and, a reproducible trip for an internal fault during a power swing. After numerous tests it could be observed that HSD-function didn't exhibit over-function also during extremely high power swing frequency, over 10Hz. The appropriate reaction of HSD during power swing for internal fault is presented in Figure 17. Before short circuit happened the significant delta-quantities for voltage and current already appear, which result from power swing phenomenon. This has naturally a negative influence on

HSD-function operation, because this method is based on delta-quantities. However, during the strong short circuit more affected delta-quantities are created that contribute to detection of the fault direction and its localization. This is shown in Figure 17. After fault the voltage u_{HSD} is higher than u_{ref}. Therefore, it is correctly concluded as an internal fault. In order to avoid the mis-operation of HSD-function during power swing some stabilization rules were designed for this network state as well. It should be noted here that effects can appear that are similar to those of faults during disturbances. Since lower frequency components appear during a power swing, the stabilization algorithm has a more static form. Moreover the relevant states of different networks were simulated and the reaction of the HSD-algorithm was investigated. These network states include switching on fault, external and internal fault clearance, frequency deviation, weak in-feed, etc.

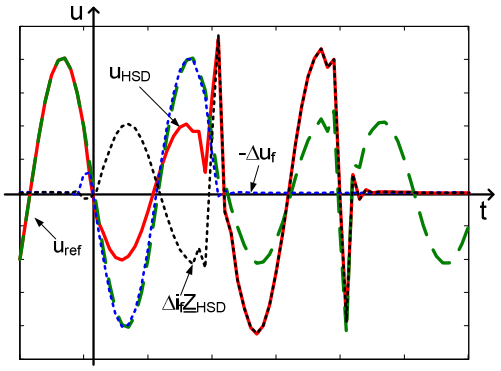

Figure 16. Evolving fault during the same phase AN reverse to AN forward

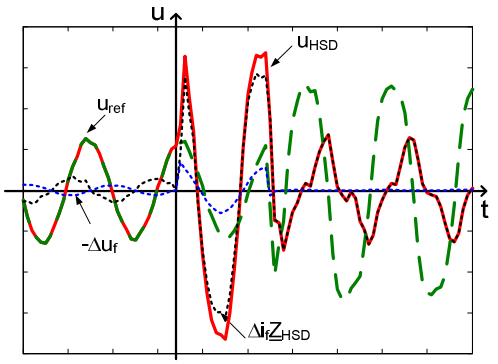

Figure 17. Internal fault during power swing

Each of these mentioned effects can have a negative influence on HSD-function. Therefore during implementation numerous stabilization and plausibility rules for detection of non conformed network operation were designed and successfully tested. The importance of such tests can be considered based on the analysis of external fault clearance process. After external fault the HSD-algorithm is picked up. Because the fault is not in the protected zone no reaction is expected. Through the external fault clearance in a short amount of time, from HSD point of view, conditions similar to those of a normal fault occur. The voltage will be recovered and current will drop rapidly down, so that big delta-quantities for these values appear. Additionally during fault clearance, relative big disturbances can be recognized, which can contribute to an over-function of the HSD-method. Therefore switching operation in the network can be dangerous for time based distance protection. Many such diverse dynamic and static network states were simulated and no over-function of HSD-algorithm was detected. Therefore, this function can be confirmed as stable. Disturbed operation of the measurement system, in addition to an undesired network state, can influence negatively the HSD-algorithm and contribute to mis-operation. These disturbances regarding measurement problem include CT saturation, CT broken or fuse failure. Extensive tests were carried out in the range of these phenomena and proper HSD-reactions were recognized.

IV. SUMMARY

In this paper the High-Speed-Distance protection function was discussed in detail. The theoretical background of the method, its sensitivity investigation as well as test results were presented. As can be concluded, this time based distance function is characterized by very good time performance and robustness. Also, the application range of the method is huge. It spreads from the simple faults through evolving faults to more complex faults during, e.g., power swing. Nevertheless, the HSD-algorithm should operate in combination with conventional distance protection because its under-function reaction can not be excluded. The HSD-algorithm exhibits under-function reaction particularly when very complex faults appear or if there is a strong deviation from the conformed network operation before the fault occurred. Therefore, HSD can not completely replace conventional distance protection, but it can operate as secure support for conventional distance protection.

REFERENCES

[1] H. Ungrad, W. Winkler and A. Wiszniewski, “Protection techniques in electrical energy systems,” Marcel Dekker, INC New York 1995.

[2] A. G. Phadke and S. H. Horowitz, “Power System Relaying,” Wiley Inc., 1995.

[3] G. Ziegler, “Numerical distance protection: principles and applications”, Publicis Corporate Publishing, 3rd edition 2008.

[4] H.-J. Herrmann, “Digitale Schutztechnik: Grundlagen, Software, Ausführungsbeispiele,“ VDE-Verlag GMBH, Berlin, Offenbach 1997.

[5] M. Vitins, “A fundamental concept for high speed relaying,” ,” IEEE Transactions on Power Apparatus and Systems, vol. 100, No. 1. pp. 163-173, January 1981.

[6] M. Chamia and S. Liberman, “Ultra high speed realy for EHV/UHV transmission lines – development, design and application,” ,” IEEE Transactions on Power Apparatus and Systems, vol. 97, No. 6. pp. 2104-2112, Nov/Dec 1978.

[7] F. Engler, O.E Lanz, M. Hanggli and G. Bacchini, “Transient signals and their processing in an ultra high-speed-directional relay for EHV/UHV transmission line protection,” IEEE Transactions on Power Apparatus and Systems, vol. 104, No. 6. pp. 1463-1473, June 1985.

[8] G. Benmouyal and S. Chano, “Characterization of the phase and amplitude comparators in UHS directional relays,” IEEE Transactions on Power Systems, vol. 12, No. 2, pp. 646-653, May 1997.

[9] G. Benmouyal, “Amplitude-independent comparators for UHS directional relays,” Developments in Power System Protection, Conference Pubplication IEE, no. 434, pp. 78-82, 25-27th March 1997.

[10] K. S. Prakash, O.P Malik and G.S Hope, “Amplitude comparator based algortihm for directional comparison protection of transmission lines,” IEEE Transactions on Power Delivery, vol. 4, No. 4, pp. 2032-2041, October 1989.